Effectiveness of reducing the influence of CTAB at the surface of metal nanoparticles during in situ heating studies by TEM

Effectiveness of reducing the influence of CTAB at the surface of metal nanoparticles during in situ heating studies by TEM.

Robin De Meyer[a,b], Wiebke Albrecht[a,b], Sara Bals[a,b]

[a] EMAT, University of Antwerp, Groenenborgerlaan 171, B-2020 Antwerp, Belgium

[b] Nanolab Centre of Excellence, Groenenborgerlaan 171, B-2020 Antwerp, Belgium

Abstract

In situ TEM is a valuable technique to offer novel insights in the behavior of nanomaterials under various conditions. However, interpretation of *in situ* experiments is not straightforward since the electron beam can impact the outcome of such measurements. For example, ligands surrounding metal nanoparticles transform into a protective carbon layer upon electron beam irradiation and may impact the apparent thermal stability during *in situ* heating experiments. In this work, we explore the effect of different treatments typically proposed to remove such ligands. We found that plasma treatment prior to heating experiments for Au nanorods and nanostars increased the apparent thermal stability of the nanoparticles, while an activated carbon treatment resulted in a decrease of the observed thermal stability. Treatment with HCl barely changed the experimental outcome. These results demonstrate the importance of carefully selecting pre-treatments procedures during *in situ* heating experiments.

Keywords — *In situ* experiments, ligands, thermal stability, transmission electron microscopy, electron beam effects, sample preparation

1 INTRODUCTION

Metallic nanoparticles (NPs) have unique functions that can differ greatly from their bulk equivalents. Because of these properties, metallic NPs have great potential for various applications. For example, in the field of life science, gold NPs can be used for molecular sensing, as contrast agents in imaging, for drug delivery applications and even as therapeutic agents (Huang et al., 2010; Stone et al., 2011; Sun et al., 2011). Metallic NPs furthermore play an important role in thermo-, electro- and photocatalysis to facilitate a multitude of reactions (Han et al., 2019; Hassanzadeh et al., 2013; Priecel et al., 2016). Unfortunately, metallic NPs are much less stable at increased temperatures in comparison to bulk Au. Indeed, whereas Au has a melting temperature of 1064 °C, anisotropic Au NPs can already deform at temperatures as low as 100 °C (Mohamed et al., 1998). Understanding the structural changes of Au NPs at high temperature is therefore of great importance for their use in future applications.

Transmission electron microscopy (TEM) is a useful technique to investigate the structure and composition of NPs. Electron tomography also enables one to perform these investigations in 3D (Weyland and Midgley, 2004). To understand the behavior of metallic NPs under conditions that are relevant for their applications, novel approaches for *in situ* experiments have been developed (Nanoscience instruments, 2020; Vanrompay et al., 2018). For example, using dedicated *in situ* holders, based on microelectromechanical system (MEMS) technology, structural, compositional and morphological changes of NPs can be studied as a function of temperature (Chatterjee et al., 2004; Vanrompay et al., 2018) or in a realistic environment such as a liquid or a gas (Altantzis et

al., 2019; Zhu et al., 2018). Recently, such experiments were combined with electron tomography to study particles in 3D (Albrecht et al., 2019; Altantzis et al., 2019; Skorikov et al., 2019; Vanrompay et al., 2018).

Although *in situ* experiments are an important addition to the TEM toolbox, one should not forget that the electron beam might influence the outcome of these measurements. As reported earlier, irradiating a Au NP by electrons might impact the *in situ* behavior (Azcárate et al., 2017) and deformation at high temperature (Albrecht et al., 2018). Clearly, this effect should be taken into account during *in situ* experiments and their interpretation. For example, it was found by Albrecht and co-workers that the CTAB surfactant surrounding the Au NPs transformed into a protective carbon layer around the NPs upon electron beam exposure, preventing the NPs to deform in inert atmospheres at temperatures up to 400 °C, although *ex situ* results showed that these particles deformed at much lower temperatures (Albrecht et al., 2018). This might lead to a wrong interpretation of the thermal stability of these particles. In order to prevent such electron beam induced effects, one could attempt to remove the surface ligands. When the particles are in colloidal solution, the surface ligands are indispensable for their stability. Removal of the surface ligands therefore needs to happen when the NPs are deposited on the TEM grid. Many techniques have already been developed to remove hydrocarbon contamination from TEM grids that originate from the grid preparation or even just the air. Contamination removal treatments typically include plasma cleaning, acid treatment and activated carbon treatment (Algara-Siller et al., 2014; Hansen et al., 2010; HAYAT, 1986; McGilvery et al., 2012; Mitchell, 2015; Pantelic et al., 2011). In this study, we will investigate if these treatments are also effective in removing organic ligands surrounding the NPs. Moreover, we want to explore in how far different sample preparation treatments can

influence *in situ* results. We will hereby focus on *in situ* heating studies and the effect of possibly remaining ligands on the deformation at high temperatures.

2 EXPERIMENTAL METHODS

2.1 Microscopy and data analysis

For all experiments, an FEI Osiris TEM was used in HAADF-STEM mode at 200 kV together with an *in situ* heating holder from DENSsolutions. The microscopy parameters were kept constant for every experiment, with a screen current of 50 pA and an electron dose of approximately 200 $e^-/Å^2$. We refer to nanoparticles as being pre-irradiated, when one 1 k x 1 k HAADF-STEM image was acquired of the region of interest under these conditions. We used Au nanorods (NRs) and Au nanostars (NSs) synthesized by seed-mediated growth with CTAB as a surfactant (Scarabelli et al., 2015; Yuan et al., 2012a, 2012b). For the *in situ* experiments, the NPs were dropcasted on a heating chip and were left to dry at room temperature. Next, multiple particles were imaged in a specific region of the heating chip. Then, the chip was heated to 100 °C and was left at that temperature for 15 minutes, after which it was quenched to room temperature. Thereafter, images of the same particles were acquired. Furthermore, particles that were not irradiated by the electron beam previously (from a different region on the heating chip) were imaged as well. These steps were then repeated for 200 °C, 300 °C and 400 °C. HAADF STEM images were processed and analyzed using the TEM Imaging & Analysis (TIA) software version 4.19.

2.2 Plasma cleaning

For the plasma treatment, the NRs and NSs were dropcasted on a heating chip in the same manner. Then, the heating chip was placed in a *Fischione Model 1070 Nanoclean* plasma cleaner for 10

minutes. A plasma was generated with pure oxygen gas and a power of 50 W was used. After plasma treatment, the same *in situ* experiment was performed as described in the previous section.

2.3 Acid treatment

For the acid treatment, a heating chip containing the NPs was submerged in a 0.25 M HCl solution for 15 minutes. After this treatment, the chip was washed multiple times with deionized water to remove all the remaining acid. After drying at room temperature, the chip was inserted in the microscope and the same experiment was performed.

2.4 Activated carbon treatment

For the activated carbon treatment, a heating chip containing the NPs was placed in a cleaned glass dish. To prevent oxidation of the electrodes on the heating chip, they were covered with parafilm. Next, a small amount of crushed activated carbon was placed on top of the heating chip with the side containing the sample facing up. Then, the dish was placed on a heating plate where it was heated to 100 °C for 30 minutes in open air. It should be noted that CTAB does not decompose at temperatures below 200 °C (Kumar et al., 2006). After that, the heating plate was switched off and the system was left to cool down for 30 minutes. Finally, the remaining activated carbon was removed from the chip using compressed air. After this treatment, the chip was inserted in the microscope and the same experiment was repeated.

3 RESULTS AND DISCUSSION

First, we will reproduce the general result of an earlier publication by Albrecht et. al., where an apparent increase in thermal stability of Au nanorods (NRs) after electron beam irradiation was observed (Albrecht et al., 2018). These results will serve as a benchmark for further experiments.

Then, the influence of plasma cleaning, acid washing and activated carbon treatment prior to *in situ* heating experiments using the same Au NPs will be investigated.

3.1 Benchmark *in situ* experiment

First, we will quantitatively compare the high temperature deformation of Au NRs and NSs that were irradiated by the electron beam prior to heating and non-irradiated particles. In Figure 1 A, a set of pre-irradiated Au NPs are shown after heating to different temperatures for 15 min. Figure 1 B shows the results of the same experiment but for Au NPs that were not irradiated prior to heating at a given temperature. These figures show that pre-irradiated Au NRs did not change notably and the pre-irradiated NSs still showed sharp features after heating at 200 °C. Even after heating at 400 °C, some anisotropy of the NSs remained. However, when the Au NPs were not irradiated prior to heating, the NSs lost almost all of their features after heating at 200 °C and no anisotropy remained after heating at 300 °C. Moreover, the non-irradiated Au NRs appeared somewhat shorter and wider at elevated temperatures. Also note that NPs sintered easily when were close to each other, forming large agglomerated that could no longer be treated as individual NPs (see Figure 1 B after heating at 300/400 °C). This limited the number of particles that could be included in the quantitative analysis, especially after heating at high temperatures.

To quantify the results, we measured morphological features of the NPs. The results are shown in Figure 1 C-D. For the Au NRs, the aspect ratio (AR) was measured, but since the highly anisotropic NSs particles yielded various morphologies, we used the diameter of the smallest possible circle that encompassed the entire NS in the 2D HAADF-STEM image as a measure for the NSs. As seen in Figure 1 A-B, when the NSs deformed, their sharp tips disappeared. Consequently, the diameter of the smallest circle containing the NS decreased for a given NS. The average AR and diameter were calculated based on at least 30 individual NRs and at least 10 individual NSs. Overlapping or

sintered/agglomerated particles were excluded from the analysis. Figure 1 C (NRs) confirms that pre-irradiated NRs deformed only slightly since the AR decreased from 3.3 ± 0.4 to 3.2 ± 0.4. However, for non-irradiated NRs the AR dropped from 3.3 ± 0.4 to 2.2 ± 0.7. The non-irradiated NSs reached a minimal diameter after heating at 200 °C, after which the particles were quasi spherical so they could not deform further. The pre-irradiated NSs remained notably more anisotropic at high temperatures. For example, after heating at 200 °C the irradiated NSs still had an average diameter of 95 ± 16 nm while the non-irradiated NSs reached the minimal average diameter of 75 ± 6 nm.

Based on the results shown in Figure 1, it is clear that the electron beam had a significant impact on the thermal stability of the Au NPs. These findings are in good agreement with the results from Albrecht et. al. (Albrecht et al., 2018). As explained by these authors, this effect is due to the formation of a protective amorphous carbon layer surrounding the NPs by pyrolysis of the CTAB ligands around the particles, consequently leading to inhibited surface diffusion and hence less deformation (Albrecht et al., 2018). In the following, we will explore in how far various sample treatments can minimize this effect allowing for a more reliable representation of the actual deformation behavior during *in situ* TEM investigations.

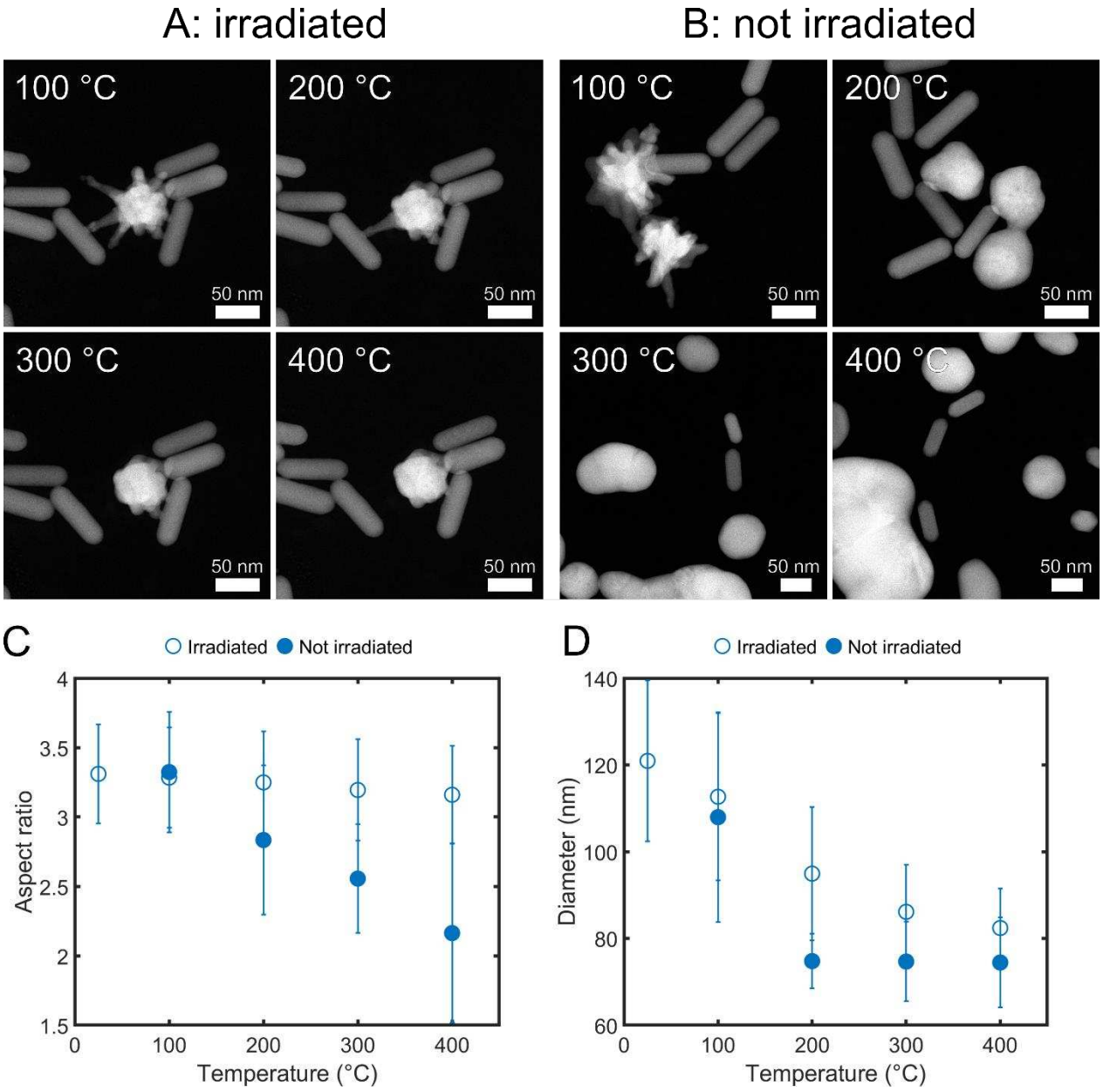

Figure 1: Influence of the electron beam during in situ heating experiments. A: HAADF STEM images of pre-irradiated Au NRs and NSs after heating to different temperatures for 15 min. B: HAADF STEM images of Au NRs and NSs on the same chip without prior electron beam irradiation. The NPs that had been irradiated prior to heating appeared more thermally stable in comparison to the non-irradiated NPs. C: Comparison of AR of untreated Au NRs with and without electron beam irradiation prior to heating. The NRs were more stable after electron

beam irradiation as is evident from the higher AR. D: Comparison of diameters of untreated Au NSs with and without electron beam irradiation prior to heating. The irradiated NSs deformed less compared to the non-irradiated NSs.

3.2 Plasma cleaning

The first treatment is based on the use of an oxygen plasma, as explained in the experimental methods section. The results are shown in Figure *2* and by comparison with Figure 1, we conclude that plasma treatment certainly had an impact on the outcome of the *in situ* heating experiments. Surprisingly, the non-irradiated plasma treated NRs (A: filled red circles) barely deformed after heating at 300 °C, showing no significant difference with the pre-irradiated NRs (A: hollow red circles). Only after heating at 400 °C a substantial deformation of the NRs was observed. In addition, the plasma treated NSs that were not irradiated before heating (B: filled red circles) even showed an increased stability at 200 °C in comparison to the non-irradiated untreated NSs (B: filled blue circles). Based on our results, it is likely that the plasma treatment affected the CTAB surfactant surrounding the particles, potentially transforming it into a carbon layer, similar to what was proposed by Albrecht and co-workers (Albrecht et al., 2018). This means that when a sample is treated with an oxygen plasma prior to an *in situ* heating microscopy experiment, instead of removing the ligands and eliminating the variations of *in situ* results, a protective layer is formed affecting the apparent thermal stability. It can be expected that the effect of a plasma treatment strongly depends on various plasma parameters, such as the composition of the gases for example. It is therefore not proven that the effects that are described here will always be identical when plasma treating the sample. However, it should be taken into account when preparing the sample. Interestingly, at 400 °C both the irradiated and non-irradiated NRs deformed more after the plasma treatment (A: red circles) compared to the non-treated particles (A: blue circles). For irradiated

NPs, this could indicate that, although the plasma transformed the CTAB into a protective layer, part of these organic compounds were also removed by the plasma. This would make the protective carbon layer thinner, meaning it could allow for a larger deformation of the NPs at higher temperatures since there is less material preventing the diffusion of the Au atoms. For non-irradiated NPs, stronger deformation of the NRs at 400 °C could indicate that part of the ligands were nonetheless removed, which might create gaps in the carbon shell allowing for easier surface diffusion of the gold atoms. However, this trend was not observed for the Au NSs or at other temperatures and might be rather related to statistical deviations.

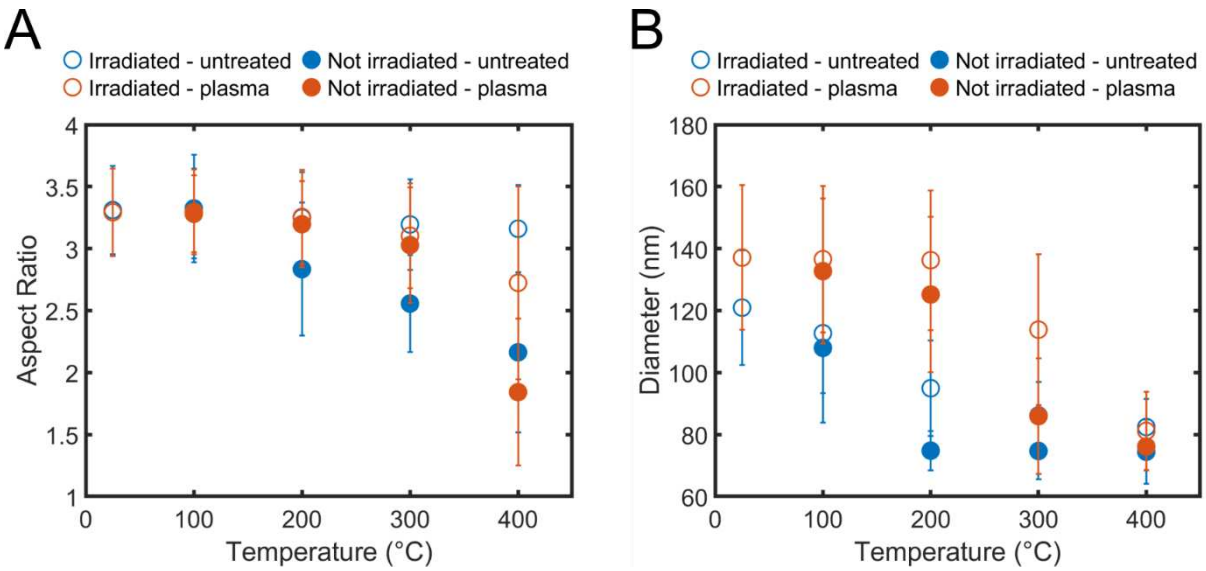

Figure 2: Influence of oxygen plasma cleaning on in situ heating experiments. A: Comparison of the AR of Au NRs treated with O2 plasma and untreated NRs. The non-irradiated plasma treated NRs remained more stable at higher temperatures (higher aspect ratio at temperatures up to 300 °C), while being equally or less stable at 400 °C compared to the untreated NRs. B: Comparison of the diameters of Au NSs treated with O2 plasma and untreated NSs. While the untreated non-irradiated NSs were already spherical after heating at 200 °C, the plasma treated non-irradiated NSs still had a larger average diameter.

3.3 Acid treatment

In the next step, we submerged the chip with the deposited Au NPs in a 0.25 M HCl solution prior to the experiment (details can be found in the Methods section). The results are shown in Figure 3. Although a slight change in deformation behavior could be observed for the NSs after heating at 100 °C, there was no significant difference between the particles that were treated with HCl and the untreated particles at all other temperatures. This shows that our acid treatment did not significantly affect the CTAB layer surrounding the NPs and that it is not useful to remove surface ligands. Since the ligands most likely remained present, the electron beam still strongly affected the outcome of the *in situ* experiment, similar to the benchmark experiment.

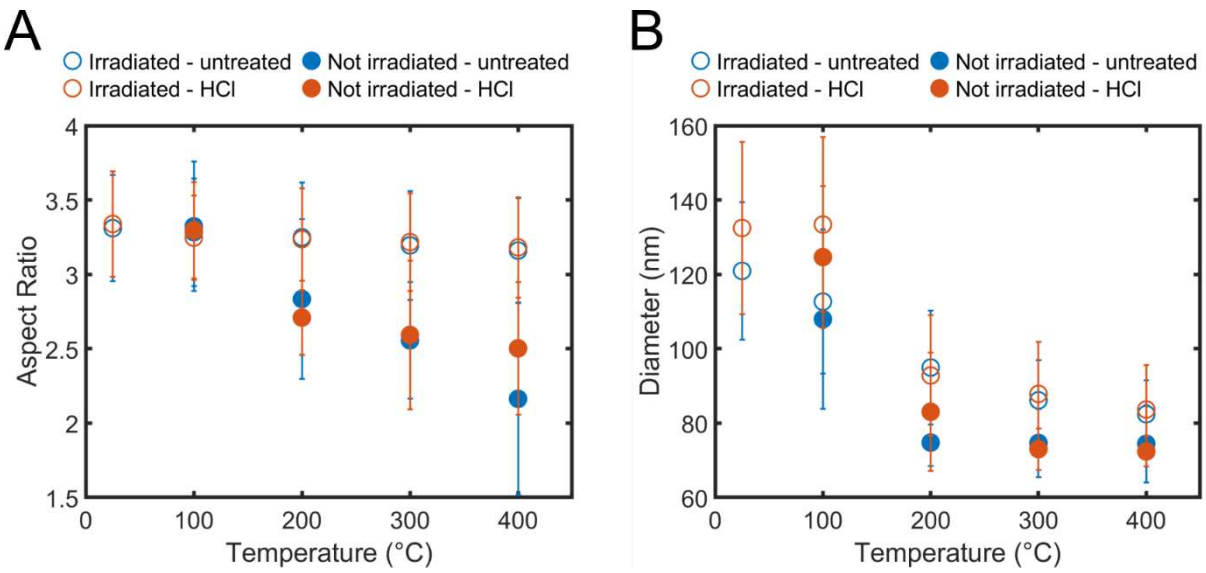

Figure 3: Influence of HCl treatment on in situ heating experiments. A: Comparison of the AR of NRs treated with HCl and untreated NRs. The effect of the acid treatment is minimal. B: Comparison of the diameters of NSs treated with HCl and untreated NSs. The effect of the acid treatment is minimal except for a slight deviation at 100 °C.

3.4 Activated carbon treatment

Finally, we treated the heating chip containing the deposited NPs with activated carbon (details can be found in the Methods section). As shown in Figure 4, the non-irradiated Au NRs and NSs (filled red circles) deformed notably more compared to non-irradiated untreated particles (filled blue circles). The aspect ratios of the NRs were substantially lower for the non-irradiated activated carbon treated particles compared to the untreated NRs for temperatures above 100 °C (Figure 4A). For the NSs, a difference was only noticeable after heating at 100 °C, because at higher temperatures, the NSs already reached their minimal diameter configuration (i. e. spherical). Note that the irradiated particles (hollow circles) behaved in the same manner, independent of pre-treatment. This shows that some of the ligands must have remained after the activated carbon treatment because the electron beam still formed the protective carbon layer. At the same time, some of the ligands were removed and/or the CTAB shell was weakened, because when the particles were not irradiated, the Au atoms could more easily diffuse across the surface, causing a greater deformation. Activated carbon has been proven to be effective in removing hydrocarbon contamination, but this technique often requires temperatures (approximately 300 °C) far too high for anisotropic NPs (Algara-Siller et al., 2014). This could explain why our treatment was only partially successful in removing the CTAB from the NPs.

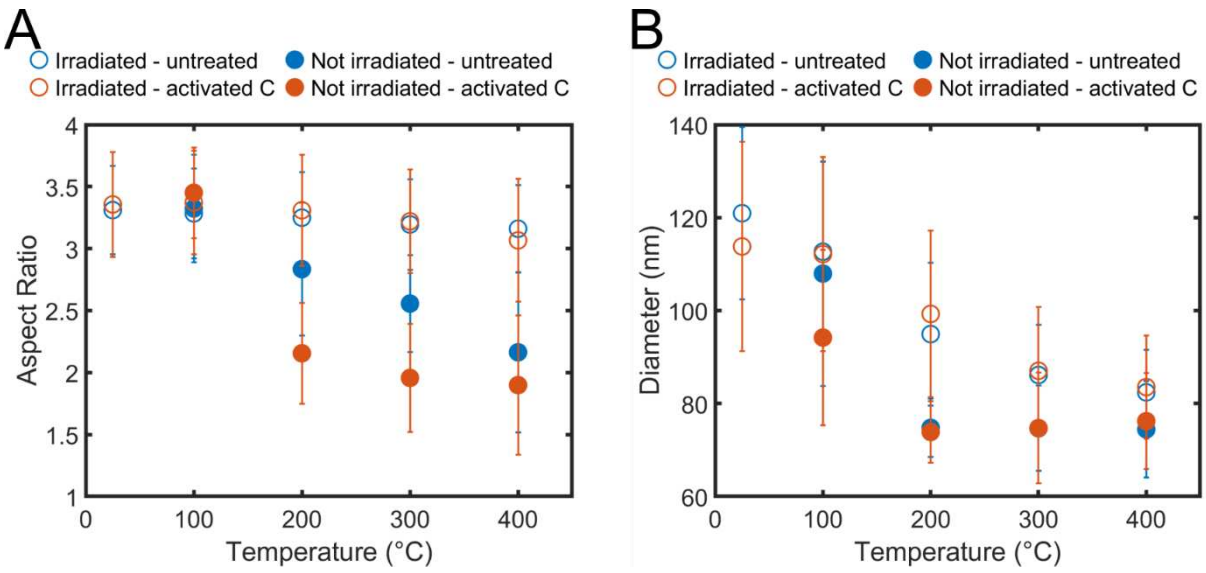

Figure 4: Influence of activated carbon treatment on in situ heating experiments. A: Comparison of the AR of Au NRs treated with activated carbon and untreated NRs. The activated carbon treated non-irradiated NRs were less stable than the untreated NRs. B: Comparison of the diameters of Au NSs treated with activated carbon and untreated NSs. Again, the activated carbon treatment made the non-irradiated particles less stable compared to the untreated ones.

While the proposed treatments did not solve the initial problem of electron beam influence on the thermal stability of Au NPs, they did imply other effects. The oxygen plasma treatment did affect the ligands, but it did not fully remove them. This is somewhat contradictory to what can be found in literature, where this technique was proven successful, so caution is needed when using plasma treatments and further research for specific plasma conditions could be valuable (Fuchs, 2009; Liu et al., 2010; Martinsson et al., 2016). The specific acid treatment used here was not successful in removing the ligands, but possibly there may be other chemical treatments that could be used in an attempt to remove these surface ligands, for example with ozone or $(NH_4)_2S$ (Choi et al., 2008; Menard et al., 2006; Sanz-Ortiz et al., 2015; Wang et al., 2010; Zhang et al., 2011). Finally, the activated carbon treatment showed promising results, but still did not entirely remove all ligands.

Further investigation and optimization of this technique might prove very useful in future sample preparation techniques for *in situ* experiments.

These results show that many processes can influence the results of *in situ* experiments. The standard techniques, often used to remove ligands were not successful. This is an important observation and demonstrates that the necessary caution should be taken when interpreting *in situ* heating results. While these experiments were only conducted using NPs with CTAB as a ligand, we believe the results are more widely applicable. As CTAB is mostly a hydrocarbon chain, we believe the presented effects are due to breaking of C-C bonds in the ligands. Therefore, these results are expected to be similar for all ligands that consist mainly of C-C bonds. Further research should be directed towards better understanding these processes for a larger variety of ligands, eventually leading to a technique that reliably removes all surface ligands without affecting the NPs. Alternatively, when the influence of the ligands is an important part of the research, experiments can better be performed *ex situ* or under low electron beam exposure. Possible techniques to minimize the electron beam exposure include the use of integrated differential phase contrast and compressed sensing. However, it still needs to be investigated whether these techniques are compatible with *in situ* studies.

4 CONCLUSION

In this paper, we confirmed that electron beam irradiation increased the apparent thermal stability of Au NPs surrounded by a surfactant (CTAB). This effect is attributed to the formation of a protective carbon layer around the NPs due to the pyrolysis of the ligands. In order to eliminate this stabilizing effect, which influences the expected behavior of the NPs at elevated temperatures, we treated the sample by plasma, acid and activated carbon prior to the *in situ* experiment. These

treatments, conventionally proposed to remove ligands, were not successful in fully removing the CTAB from the NPs. Treatment by an oxygen plasma increased the apparent thermal stability of the NPs, even when they were not irradiated by the electron beam. Treatment with HCl under the conditions used in this study did not have a significant effect. Finally, activated carbon treatment showed promising results, but was still unable to fully remove all ligands.

In conclusion, we showed that the ligands can play a huge role during *in situ* experiments and various treatments that are commonly used in sample preparation can influence the outcome of an experiment due to their impact on these surface ligands. Therefore, caution is needed when performing such *in situ* heating experiments and comparison of experiments are necessary.

5 ACKNOWLEDGEMENTS

Funding: This work was supported by the European Union's Horizon 2020 research and innovation program [grant agreement No 731019 (EUSMI) and No 815128 (REALNANO)].

We acknowledge Prof. Luis M. Liz-Marzán and co-workers of the Bionanoplasmonics Laboratory, CICbiomaGUNE, Spain for providing the Au nanoparticles.

6 REFERENCES

Albrecht, W., Bladt, E., Vanrompay, H., Smith, J.D., Skrabalak, S.E., Bals, S., 2019. Thermal Stability of Gold/Palladium Octopods Studied in Situ in 3D: Understanding Design Rules for Thermally Stable Metal Nanoparticles. ACS Nano 13, 6522–6530. https://doi.org/10.1021/acsnano.9b00108

Albrecht, W., van de Glind, A., Yoshida, H., Isozaki, Y., Imhof, A., van Blaaderen, A., de Jongh, P.E., de Jong, K.P., Zečević, J., Takeda, S., 2018. Impact of the electron beam on the thermal stability of gold nanorods studied by environmental transmission electron microscopy. Ultramicroscopy 193, 97–103. https://doi.org/10.1016/j.ultramic.2018.05.006

Algara-Siller, G., Lehtinen, O., Turchanin, A., Kaiser, U., 2014. Dry-cleaning of graphene. Appl. Phys. Lett. 104, 153115. https://doi.org/10.1063/1.4871997

Altantzis, T., Lobato, I., De Backer, A., Béché, A., Zhang, Y., Basak, S., Porcu, M., Xu, Q., Sánchez-Iglesias, A., Liz-Marzán, L.M., Van Tendeloo, G., Van Aert, S., Bals, S., 2019. Three-Dimensional Quantification of the Facet Evolution of Pt Nanoparticles in a Variable Gaseous Environment. Nano Lett. 19, 477–481. https://doi.org/10.1021/acs.nanolett.8b04303

Azcárate, J.C., Fonticelli, M.H., Zelaya, E., 2017. Radiation Damage Mechanisms of Monolayer-Protected Nanoparticles via TEM Analysis. J. Phys. Chem. C 121, 26108–26116. https://doi.org/10.1021/acs.jpcc.7b08525

Chatterjee, K., Howe, J.M., Johnson, W.C., Murayama, M., 2004. Static and in situ TEM investigation of phase relationships, phase dissolution, and interface motion in Ag–Au–Cu alloy nanoparticles. Acta Materialia 52, 2923–2935. https://doi.org/10.1016/j.actamat.2004.02.038

Choi, B.-S., Iqbal, M., Lee, T., Kim, Y., Tae, G., 2008. Removal of Cetyltrimethylammonium Bromide to Enhance the Biocompatibility of Au Nanorods Synthesized by a Modified Seed Mediated Growth Process. Journal of nanoscience and nanotechnology 8, 4670–4. https://doi.org/10.1166/jnn.2008.IC18

Fuchs, P., 2009. Low-pressure plasma cleaning of Au and PtIr noble metal surfaces. Applied Surface Science 256, 1382–1390. https://doi.org/10.1016/j.apsusc.2009.08.093

Han, C., Qi, M.-Y., Tang, Z.-R., Gong, J., Xu, Y.-J., 2019. Gold nanorods-based hybrids with tailored structures for photoredox catalysis: fundamental science, materials design and applications. Nano Today 27, 48–72. https://doi.org/10.1016/j.nantod.2019.05.001

Hansen, T.W., Wagner, J.B., Dunin-Borkowski, R.E., 2010. Aberration corrected and monochromated environmental transmission electron microscopy: challenges and prospects for materials science. Materials Science and Technology 26, 1338–1344. https://doi.org/10.1179/026708310X12756557336355

Hassanzadeh, J., Amjadi, M., Manzoori, J.L., Sorouraddin, M.H., 2013. Gold nanorods-enhanced rhodamine B-permanganate chemiluminescence and its analytical application. Spectrochimica Acta Part A: Molecular and Biomolecular Spectroscopy 107, 296–302. https://doi.org/10.1016/j.saa.2013.01.068

HAYAT, M.A., 1986. 4 - Positive Staining, in: HAYAT, M.A. (Ed.), Basic Techniques for Transmission Electron Microscopy. Academic Press, pp. 182–231. https://doi.org/10.1016/B978-0-12-333926-3.50007-5

Huang, X., El-Sayed, I.H., El-Sayed, M.A., 2010. Applications of Gold Nanorods for Cancer Imaging and Photothermal Therapy, in: Grobmyer, S.R., Moudgil, B.M. (Eds.), Cancer Nanotechnology: Methods and Protocols. Humana Press, Totowa, NJ, pp. 343–357. https://doi.org/10.1007/978-1-60761-609-2_23

Kumar, R., Chen, H.-T., Escoto, J.L.V., Lin, V.S.-Y., Pruski, M., 2006. Template Removal and Thermal Stability of Organically Functionalized Mesoporous Silica Nanoparticles. Chem. Mater. 18, 4319–4327. https://doi.org/10.1021/cm060598v

Liu, Y., Pan, Y., Wang, Z.-J., Kuai, P., Liu, C.-J., 2010. Facile and fast template removal from mesoporous MCM-41 molecular sieve using dielectric-barrier discharge plasma. Catalysis Communications 11, 551–554. https://doi.org/10.1016/j.catcom.2009.12.017

Martinsson, E., Shahjamali, M.M., Large, N., Zaraee, N., Zhou, Y., Schatz, G.C., Mirkin, C.A., Aili, D., 2016. Influence of Surfactant Bilayers on the Refractive Index Sensitivity and Catalytic Properties of Anisotropic Gold Nanoparticles. Small 12, 330–342. https://doi.org/10.1002/smll.201502449

McGilvery, C.M., Goode, A.E., Shaffer, M.S.P., McComb, D.W., 2012. Contamination of holey/lacey carbon films in STEM. Micron 43, 450–455. https://doi.org/10.1016/j.micron.2011.10.026

Menard, L.D., Xu, F., Nuzzo, R.G., Yang, J.C., 2006. Preparation of TiO2-supported Au nanoparticle catalysts from a Au13 cluster precursor: Ligand removal using ozone exposure versus a rapid thermal treatment. Journal of Catalysis 243, 64–73. https://doi.org/10.1016/j.jcat.2006.07.006

Mitchell, D.R.G., 2015. Contamination mitigation strategies for scanning transmission electron microscopy. Micron 73, 36–46. https://doi.org/10.1016/j.micron.2015.03.013

Mohamed, M.B., Ismail, K.Z., Link, S., El-Sayed, M.A., 1998. Thermal Reshaping of Gold Nanorods in Micelles. J. Phys. Chem. B 102, 9370–9374. https://doi.org/10.1021/jp9831482

Nanoscience instruments, 2020. In-Situ TEM: State-of-the-art Research + Conventional TEM [WWW Document]. URL https://www.nanoscience.com/products/tem-sample-holders/ (accessed 10.18.20).

Pantelic, R.S., Suk, J.W., Magnuson, C.W., Meyer, J.C., Wachsmuth, P., Kaiser, U., Ruoff, R.S., Stahlberg, H., 2011. Graphene: Substrate preparation and introduction. Journal of Structural Biology 174, 234–238. https://doi.org/10.1016/j.jsb.2010.10.002

Priecel, P., Adekunle Salami, H., Padilla, R.H., Zhong, Z., Lopez-Sanchez, J.A., 2016. Anisotropic gold nanoparticles: Preparation and applications in catalysis. Chinese Journal of Catalysis 37, 1619–1650. https://doi.org/10.1016/S1872-2067(16)62475-0

Sanz-Ortiz, M.N., Sentosun, K., Bals, S., Liz-Marzán, L.M., 2015. Templated Growth of Surface Enhanced Raman Scattering-Active Branched Gold Nanoparticles within Radial Mesoporous Silica Shells. ACS Nano 9, 10489–10497. https://doi.org/10.1021/acsnano.5b04744

Scarabelli, L., Sánchez-Iglesias, A., Pérez-Juste, J., Liz-Marzán, L.M., 2015. A “Tips and Tricks” Practical Guide to the Synthesis of Gold Nanorods. J. Phys. Chem. Lett. 6, 4270–4279. https://doi.org/10.1021/acs.jpclett.5b02123

Skorikov, A., Albrecht, W., Bladt, E., Xie, X., van der Hoeven, J.E.S., van Blaaderen, A., Van Aert, S., Bals, S., 2019. Quantitative 3D Characterization of Elemental Diffusion Dynamics in Individual Ag@Au Nanoparticles with Different Shapes. ACS Nano 13, 13421–13429. https://doi.org/10.1021/acsnano.9b06848

Stone, J., Jackson, S., Wright, D., 2011. Biological applications of gold nanorods. WIREs Nanomedicine and Nanobiotechnology 3, 100–109. https://doi.org/10.1002/wnan.120

Sun, H., Yuan, Q., Zhang, B., Ai, K., Zhang, P., Lu, L., 2011. GdIII functionalized gold nanorods for multimodal imaging applications. Nanoscale 3, 1990–1996. https://doi.org/10.1039/C0NR00929F

Vanrompay, H., Bladt, E., Albrecht, W., Béché, A., Zakhozheva, M., Sánchez-Iglesias, A., Liz-Marzán, L.M., Bals, S., 2018. 3D characterization of heat-induced morphological changes of Au nanostars by fast in situ electron tomography. Nanoscale 10, 22792–22801. https://doi.org/10.1039/C8NR08376B

Wang, Z., Zong, S., Yang, J., Song, C., Li, J., Cui, Y., 2010. One-step functionalized gold nanorods as intracellular probe with improved SERS performance and reduced cytotoxicity. Biosensors and Bioelectronics 26, 241–247. https://doi.org/10.1016/j.bios.2010.06.032

Weyland, M., Midgley, P.A., 2004. Electron tomography. Materials Today 7, 32–40. https://doi.org/10.1016/S1369-7021(04)00569-3

Yuan, H., Khoury, C., Fales, A., Wilson, C., Grant, G., Vo-Dinh, T., 2012a. Plasmonic Gold Nanostars: A Potential Agent for Molecular Imaging and Cancer Therapy, in: Biomedical Optics and 3-D Imaging, OSA Technical Digest. Presented at the Biomedical Optics and 3-D Imaging, Optical Society of America, Miami, Florida, p. BM2A.8. https://doi.org/10.1364/BIOMED.2012.BM2A.8

Yuan, H., Khoury, C.G., Hwang, H., Wilson, C.M., Grant, G.A., Vo-Dinh, T., 2012b. Gold nanostars: surfactant-free synthesis, 3D modelling, and two-photon photoluminescence imaging. Nanotechnology 23, 075102. https://doi.org/10.1088/0957-4484/23/7/075102

Zhang, H., Hu, B., Sun, L., Hovden, R., Wise, F.W., Muller, D.A., Robinson, R.D., 2011. Surfactant Ligand Removal and Rational Fabrication of Inorganically Connected Quantum Dots. Nano Lett. 11, 5356–5361. https://doi.org/10.1021/nl202892p

Zhu, C., Liang, S., Song, E., Zhou, Y., Wang, W., Shan, F., Shi, Y., Hao, C., Yin, K., Zhang, T., Liu, J., Zheng, H., Sun, L., 2018. In-situ liquid cell transmission electron microscopy investigation on oriented attachment of gold nanoparticles. Nature Communications 9, 421. https://doi.org/10.1038/s41467-018-02925-6